AIP | Applied Physics Letters

Impact of reduced dimensionality on the magnetic and magnetocaloric response of La0.7Ca0.3MnO3

P. Lampen, N. S. Bingham, M. H. Phan, H. Kim, M. Osofsky et al.

Citation: Appl. Phys. Lett. **102**, 062414 (2013); doi: 10.1063/1.4792239
View online: http://dx.doi.org/10.1063/1.4792239
View Table of Contents: http://apl.aip.org/resource/1/APPLAB/v102/i6
Published by the American Institute of Physics.

Related Articles

Correlation between structural parameters and the magnetocaloric effect in epitaxial La0.8Ca0.2MnO3/LaAlO3 thin film
J. Appl. Phys. 113, 063508 (2013)

Elastocaloric and magnetocaloric effects in Ni-Mn-Sn(Cu) shape-memory alloy
J. Appl. Phys. 113, 053506 (2013)

Shape-anisotropic heterogeneous nucleation and magnetic Gibbs-Thomson effect in itinerant-electron metamagnetic transition of La(Fe0.88Si0.12)13 magnetocaloric compound
Appl. Phys. Lett. 102, 041913 (2013)

Near-room-temperature refrigeration through voltage-controlled entropy change in multiferroics
Appl. Phys. Lett. 102, 031915 (2013)

Resistivity, specific heat, and magnetocaloric effect of La0.8Ag0.1MnO3: Effect of isotopic substitution of 16O→18O
Appl. Phys. Lett. 102, 032404 (2013)

Additional information on Appl. Phys. Lett.

Journal Homepage: http://apl.aip.org/
Journal Information: http://apl.aip.org/about/about_the_journal
Top downloads: http://apl.aip.org/features/most_downloaded
Information for Authors: http://apl.aip.org/authors

ADVERTISEMENT

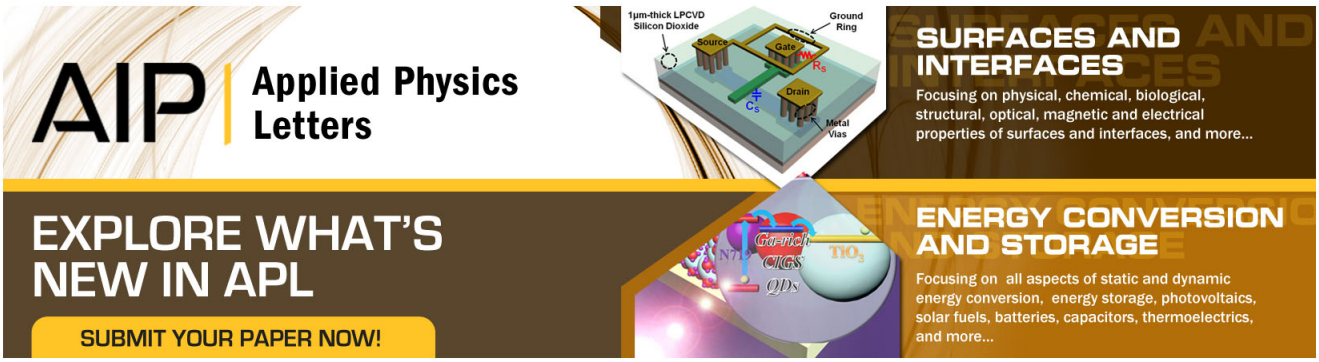

Impact of reduced dimensionality on the magnetic and magnetocaloric response of $La_{0.7}Ca_{0.3}MnO_3$

P. Lampen,[1] N. S. Bingham,[1,2] M. H. Phan,[1,a)] H. Kim,[2] M. Osofsky,[2] A. Piqué,[2] T. L. Phan,[3] S. C. Yu,[3,a)] and H. Srikanth[1,a)]
[1]*Department of Physics, University of South Florida, Tampa, Florida 33620, USA*
[2]*Naval Research Laboratory, 4555 Overlook Ave., SW, Washington DC 20375, USA*
[3]*Department of Physics, Chungbuk National University, Cheongju 361-763, South Korea*

(Received 2 January 2013; accepted 31 January 2013; published online 13 February 2013)

Understanding the impact of reduced dimensionality on the magnetic and magnetocaloric responses of a material is vital in incorporating it as an active magnetic refrigerant in cooling devices. By contrasting the magnetic and magnetocaloric behaviors of bulk polycrystalline, sol-gel derived nanocrystalline, and pulsed laser deposited thin film forms of the $La_{0.7}Ca_{0.3}MnO_3$ system, we show that reducing the dimensionality of a ferromagnetic material tends to broaden and shift the paramagnetic to ferromagnetic transition to lower temperatures, while decreasing the saturation magnetization and the magnitude of the magnetic entropy change. Relative to its bulk counterpart, a pronounced broadening of the magnetic entropy change peak in the thin film leads to enhanced refrigerant capacity—an important figure-of-merit for active magnetic refrigeration technology. With reduced dimensionality, universal curves based on re-scaled entropy change curves tend toward collapse, indicating a weakening of the first order nature of the transition in the nanocrystalline samples and a crossover to second order in the thin film. © *2013 American Institute of Physics*. [http://dx.doi.org/10.1063/1.4792239]

The push for diversified energy sources has led to a renewed focus on magnetic materials to meet the requirements for the next generation of generators and turbines and to find alternative technologies for energy-intensive applications, among them refrigeration. Recent advances in the field of permanent magnets have demonstrated that manipulating the microstructure of known materials can lead to gains in performance.[1] However, the effect of morphology on the performance of materials under consideration for magnetic cooling applications is less well understood. One such class of candidate materials are the mixed-valent manganite compounds, whose rich phase diagrams have fueled a great deal of research over the past two decades.[2] In the doping range $0.25 < x < 0.33$, $La_{1-x}Ca_xMnO_3$ exhibits a paramagnetic to ferromagnetic (PM-FM) transition between 230 K and 260 K concurrent with the insulator to metal transition. This critical temperature and doping range are characterized by colossal magnetoresistance (CMR) and a large magnetocaloric effect (MCE), prompting many studies focused on understanding the underlying transport and magnetic properties in thin films,[3–8] bulk,[9,10] and nanocrystalline[11–14] variations of $La_{1-x}Ca_xMnO_3$.

The properties of thin films as compared to their bulk counterparts vary widely depending on thickness, substrate, details of deposition, annealing, oxygen content, etc. However, the general trend upon thickness reduction is a suppression of the Curie temperature (T_C) and saturation magnetization (M_S), and an enhancement of resistivity and magnetoresistance (MR).[7] In very thin coherently strained films, disagreement exists as to whether these effects can be attributed primarily to strain or finite size effects.[5,8] In moderately thick films (>100 nm), these features are likely disorder-induced as strain relaxation can give rise to extrinsic defects such as dislocations, stacking faults, cationic vacancies, and grain boundaries.[3,4,7] Size reduction in manganite nanoparticles has also resulted in reduced T_C and M_S.[12,13] Experimental data agree well with models predicting a core/shell morphology in which the shell consists of a magnetically dead or spin glass-like surface layer, with the effect of reducing the magnetization.[11,15] Meanwhile, finite size effects (cutoff of the correlation length) in the magnetic core of the particle contribute to the suppression of T_C.[14]

To our knowledge, no study has been carried out with a side-by-side comparison of the effects of extrinsic disorder in thin films and finite size effects in nanoparticles on the magnetic and magnetocaloric properties of a single ferromagnetic manganite system. In this work, we examine the re-structuring of the first-order ferromagnetic $La_{0.7}Ca_{0.3}MnO_3$ (LCMO) compound in two forms (thin film and nanocrystalline) and compare the results with a bulk polycrystalline sample. The magnetic and magnetocaloric properties of each sample are characterized, and it is found that while the greatest deviation from the bulk behavior occurs in the thin film, the changes result in an enhanced refrigerant capacity (RC). Universal scaling based on magnetic entropy change curves is applied to understand the impact of reduced dimensionality on the nature of the ferromagnetic transition in $La_{0.7}Ca_{0.3}MnO_3$.

Samples of LCMO in various forms were prepared for comparison. LCMO thin films (~150 nm thickness) were deposited on MgO (100) substrates, from a commercially purchased stoichiometric polycrystalline target, using a KrF excimer laser (Lambda Physik LPX 305, $\lambda = 248$ nm, FWHM = 30 ns). Details of deposition techniques are described elsewhere.[16] Films were deposited at a substrate temperature of 700 °C in an oxygen pressure of 300 mTorr

a)Authors to whom correspondence should be addressed. Electronic addresses: phanm@usf.edu, scyu@chungbuk.ac.kr and sharihar@usf.edu.

 © 2013 American Institute of Physics

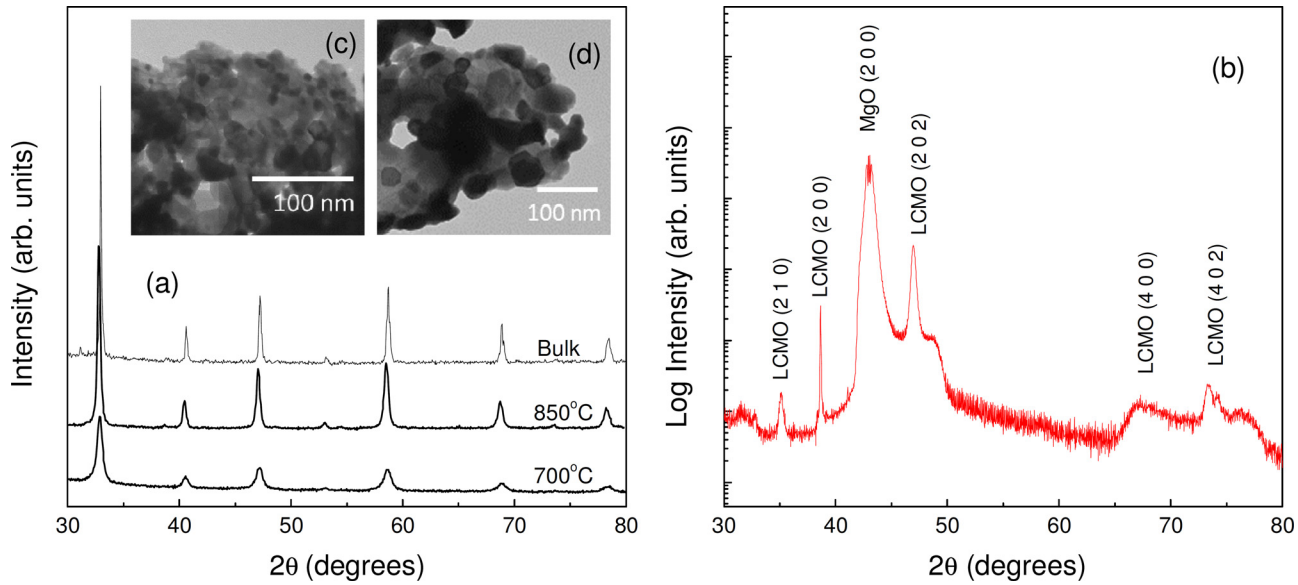

FIG. 1. (a) XRD patterns for bulk and sol-gel derived $La_{0.7}Ca_{0.3}MnO_3$ powders calcined at 700 °C and 850 °C; (b) XRD pattern for a LCMO film deposited on MgO. Insets (c) and (d) show representative TEM micrographs for nanopowders treated at 700 °C and 850 °C, respectively.

followed by annealing at 600 °C for 30 min. To minimize the effects of variation in stoichiometry and purity, a portion of the same target was used as the bulk polycrystalline reference sample while conducting magnetic measurements. A sol-gel chemical method was utilized in the preparation of the nanocrystalline materials. After stoichiometric mixing of the precursor metal nitrate solutions, citric acid was added as a polymerizing agent and the gel obtained after gradual evaporation of the solvent at 90 °C was decomposed to form a black porous powder at 150 °C. Following overnight calcination at 400 °C, the powder was divided and treated at 700 °C and 850 °C for 4 h to form nano-sized crystallites.

X-ray diffraction (XRD) patterns show the expected orthorhombic (Pnma) structure in the powders (Fig. 1(a)) and a 150 nm film (Fig. 1(b)). The absence of impurity phases was confirmed through profile matching with the FULLPROF software package, and little change was observed in the structural parameters with cell volume varying less than 0.2% between the bulk sample and the smallest particles. The morphology of the nanopowders was examined using transmission electron microscopy (TEM), which revealed mean diameters of 15 nm and 33 nm for calcination temperatures of 700 °C and 850 °C, respectively (Figs. 1(c) and 1(d)). Good agreement was found between the observed particle size and the average crystallite size determined from the XRD patterns, indicating that the individual particles are single crystalline. Magnetic measurements were carried out from 25 K to 350 K under fields up to 5 T using a commercial Quantum Design Physical Properties Measurement System (PPMS) with a vibrating sample magnetometer (VSM) attachment. The diamagnetic contribution from the MgO substrate was corrected for using a linear fitting and subtraction method.

Figure 2 shows the temperature dependence of magnetization in a polycrystalline bulk sample, nanocrystalline powders, and a thin film of $La_{0.7}Ca_{0.3}MnO_3$. Two effects are immediately obvious from inspection of the results: First, the sharp PM-FM transition that occurs in the bulk material is broadened in the samples with lower dimensionality. Secondly, the T_C—estimated here from the minima in the derivative of magnetization with temperature—shifts to lower temperatures from 264 K in the bulk to 260 K in the 33 nm powders, 241 K in the 15 nm powders and 235 K in the thin film. The broadening phenomenon can be attributed to the distribution of T_C owing to polydispersity in the nanoparticle system and local variation of strain near grain boundaries and defects in the thin film.[3,6] In a percolative system, the distribution in transition temperature is Gaussian with a width that can be qualitatively linked to the disorder present.[6] A Gaussian fit to the dM/dT curves in the inset of Fig. 2 yields distribution widths of $\Gamma = 5$ K, 9 K, 41 K, and 38 K for the polycrystalline, 33 nm, 15 nm, and thin film samples, respectively. This suggests that there is considerably more local variation in environment in the film than is induced by particle size distribution in a sub-100 nm ensemble. It is not until the mean particle size reaches 15 nm that the width of the transition in the nanocystalline system becomes comparable to that of the film which has a characteristic dimension

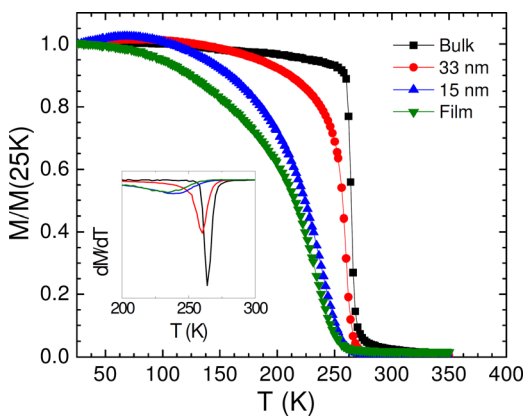

FIG. 2. Temperature dependence of magnetization recorded on cooling in a field of 500 Oe and normalized to 25 K value. Lines are guide to the eye. Inset: First derivative of magnetization.

ten times greater (~150 nm). The reduction in the average value of T_C has been observed before in both nanocrystalline and thin film forms of LCMO, and is usually attributed to finite size effects and disorder.[7,14]

To evaluate the magnetic entropy change in the system, isothermal magnetization vs. field ($M(H)$) curves were recorded around the transition temperature in each sample. The inset of Fig. 3 compares the $M(H)$ isotherms at 120 K. The 5 T value of magnetization reaches 3.5 μ_B, 2.9 μ_B, 2.4 μ_B, and 2.2 μ_B in the polycrystal, 33 nm particles, thin film, and 15 nm particles, respectively. The expected spin-only magnetic moment is determined by the Ca^{2+}-doping-dependent ratio of Mn^{4+} ($S = 3/2$) to high-spin Mn^{3+} ($S = 2$), which predicts a value of $M_0 = 3.7\ \mu_B$ in $La_{0.7}Ca_{0.3}MnO_3$. Defects and oxygen off-stoichiometry could reasonably account for the ~5% discrepancy between the polycrystalline sample and the ideal value. Although the nature and volume fraction of magnetically disordered regions in the samples with reduced dimension cannot be known precisely, we note based on a simple geometrical argument that the thickness of a dead layer ($M = 0$) at the surface of a fully magnetized spherical particle ($M = M_0$) required to reduce the magnetization to the observed values of 2.9 μ_B and 2.2 μ_B would be 1.3 nm in the 33 nm particles and 1.2 nm in the 15 nm particles, in reasonable agreement with the previous estimates.[14,17]

The entropy change in the system is obtained by integrating between successive $M(H)$ isotherms according to the thermodynamic Maxwell relation

$$\Delta S_M = \mu_0 \int_0^{H_{max}} \left(\frac{\partial M}{\partial T}\right) dH. \quad (1)$$

Under an applied field change of 5 T, the absolute value of the magnetic entropy change ($|\Delta S_M|$) reaches a peak value near the Curie temperature of 7.7 J/kg K in the polycrystalline sample. This value is in good agreement with Ref. 13, in which a sol-gel method combined with high temperature sintering was used to prepare the sample, in contrast to Ref. 10 in which a modified solid state reaction process gave rise to unusually large values of $|\Delta S_M|$ (9.9 J/kg K for $\mu_0\Delta H = 5$ T). In the nanocrystalline samples, the sensitive dependence of the magnetocaloric effect on synthesis details is even more evident: the present $|\Delta S_M|$ value of 4.9 J/kg K is more than an order of magnitude greater than the previous value reported for similarly sized particles subject to a comparable field change.[13] In the 15 nm particles, the peak value of entropy change is a factor of two smaller as the broadening of the transition and reduced magnetization become significant. The decline in the peak $|\Delta S_M|$ from the bulk sample to the nanocrystalline and thin film samples is consistent with the fall off in the magnitude of magnetic moment and the broadening of the FM-PM transition that reduces $\partial M/\partial T$ in Eq. (1).

Figure 3(b) shows the field dependence of the RC. The RC, given by $-\int_{T_1}^{T_2} \Delta S_M(T)dT$, where T_1 and T_2 are the temperatures defining the full width at half maximum, is a measure of the heat exchanged between the hot and cold ends of an ideal refrigeration cycle. The RC is considered to be an important figure of merit in the evaluation of a magnetocaloric material. It has been observed on a number of occasions that the reduced maximum value of $|\Delta S_M|$ that often accompanies broad magnetic entropy change peaks can be compensated for by the increased width, resulting in an enhanced RC over sharper transitions.[18] It can be seen that this scenario holds true in the present case: the RC is reduced in the nanocrystalline samples but reaches its largest values in the thin film for which the breadth of the transition overcomes the deleterious effects of the drop in ΔS_M. From the point of view of magnetic refrigeration, thin films show a number of desirable traits and may be particularly well-suited to cooling integrated circuits and MEMS systems. In addition to enhanced RC values as demonstrated in this study, films have the advantage of reducing material requirements while improving the maximum refrigeration cycling frequency.[19] Recently, the coupling of the second order Curie transition in LCMO with the first order structural transition on a BTO substrate was found to produce a giant reversible magnetocaloric effect.[20] On the other hand, particle size reduction down to the nanoscale in conventional ferromagnetic materials increasingly degrades magnetocaloric performance because although the transition broadens as in the case of the films, the magnetically dead surface layer eventually accounts for a significant portion of the total sample volume.

A new criterion for determining the order of a transition has recently been proposed based on a re-scaling of entropy change curves.[21] Universal behavior manifested in the collapse of ΔS_M(T) curves after a scaling procedure has been established for materials undergoing a second order magnetic transition. However, the scaling assumptions that

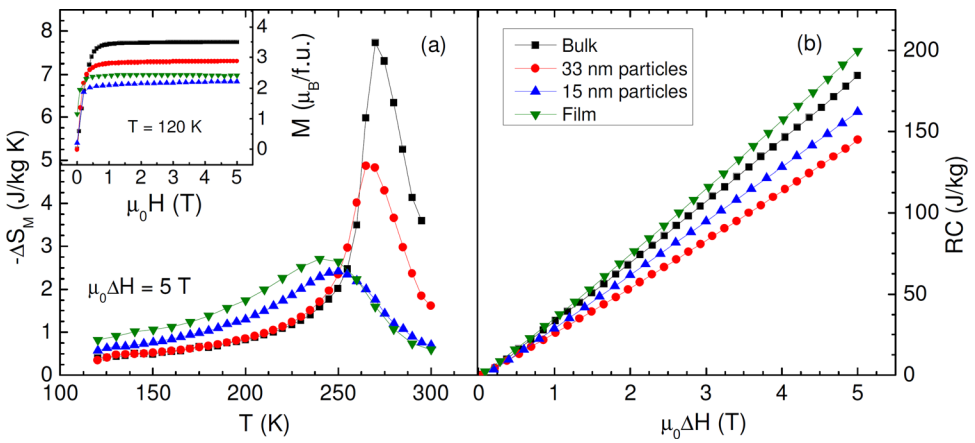

FIG. 3. (a) Comparison of temperature-dependent entropy change in bulk, nanocrystalline, and thin film $La_{0.7}Ca_{0.3}MnO_3$ samples under an applied field change of 5 T. Inset: Isothermal magnetization curves for each sample at 120 K. Lines are guide to the eye. (b) Refrigerant capacity as a function of applied magnetic field.

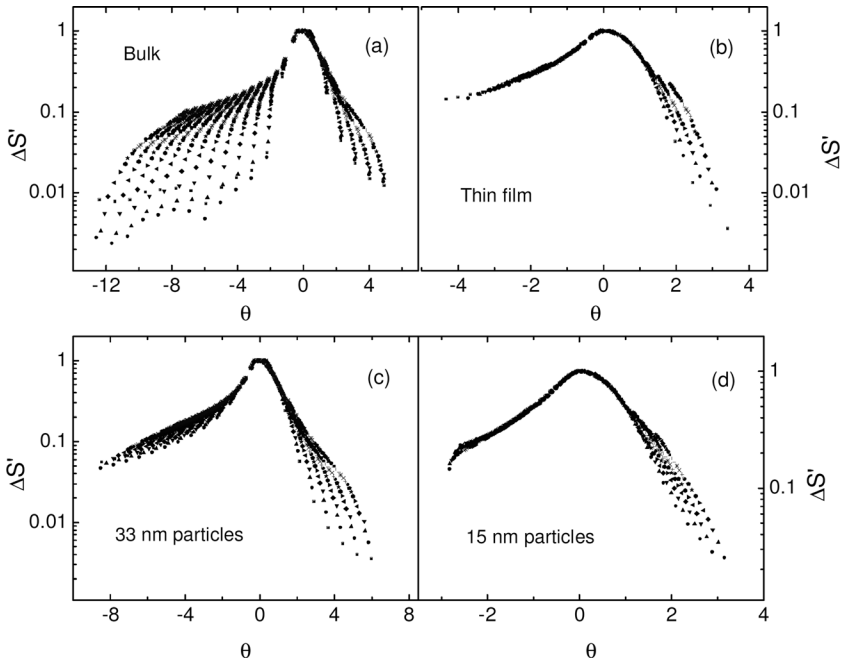

FIG. 4. Universal curve calculations as described in the text for the (a) polycrystalline bulk, (b) thin film, (c) 33 nm, and (d) 15 nm forms of $La_{0.7}Ca_{0.3}MnO_3$. Color gradient (dark to light) corresponds to field strength (low to high).

underlie this behavior break down when applied to a first order magnetic transition, and collapse of the modified $\Delta S_M(T)$ curves fails. As a consequence, whether or not collapse is achieved can be applied as a method of distinguishing first and second order magnetic transitions. Figure 4 compares the universal curve constructions for each sample by plotting $\Delta S'$ against θ, where $\Delta S' = \Delta S_M/\Delta S_M^{max}$ is the rescaled entropy change and θ is the temperature variable defined by

$$\theta = \begin{cases} -(T - T_C)/(T_{r1} - T_C) & T \le T_C \\ (T - T_C)/(T_{r2} - T_C) & T \ge T_C \end{cases}.$$

Here, the reference temperatures T_{r1} and T_{r2} are chosen such that $\Delta S_M(T_{r1}) = \Delta S_M(T_{r2}) = \Delta S_M^{max}/2$. In Fig. 4(a), the divergence of the curves is clear in the polycrystalline compound, particularly above the T_C. In the 33 nm sample, divergence is still evident indicating the first-order quality of the transition, though weaker than that of the bulk sample. In the film and the smallest particle size, there is a clear collapse of the curves below T_C, consistent with a second order transition. We note that there is not perfect agreement of the data above T_C, however a check of the Arrott plot constructions (Fig. 5) confirmed the second order nature of the transitions in these samples. The essential region for collapse to determine the order of the transition is $\theta < -1$, as collapse occurs

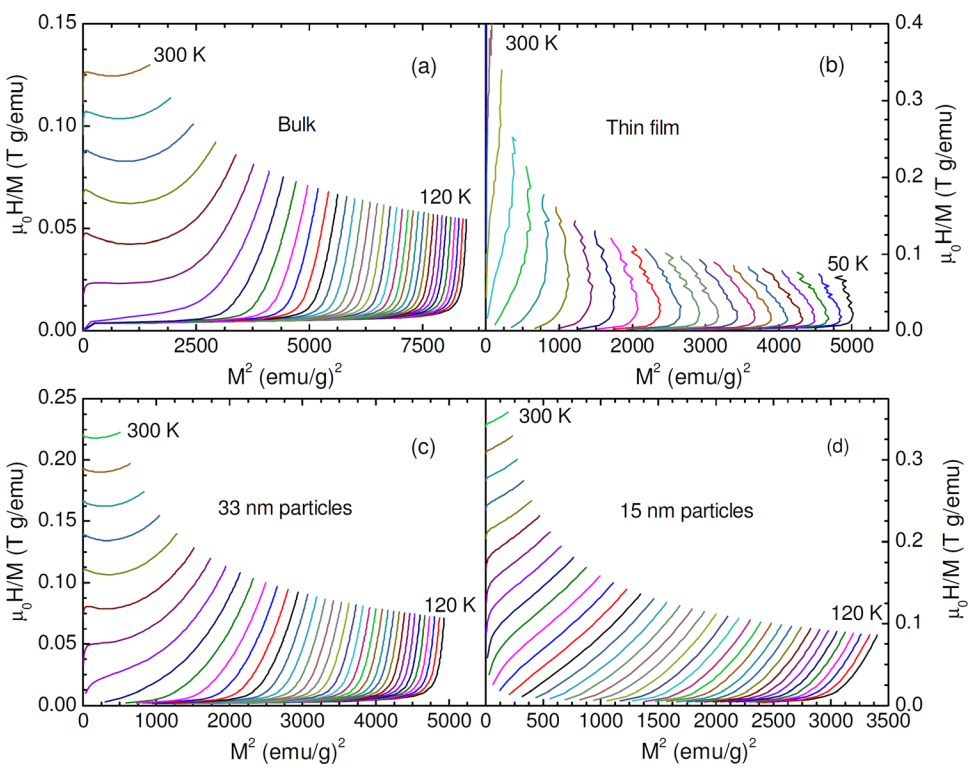

FIG. 5. Arrott plot constructions for (a) polycrystalline bulk, (b) thin film, (c) 33 nm particles, and (d) 15 nm particles.

in the range $-1 < \theta < 0$ by construction and is due to paramagnetic behavior for $\theta > 0$.[22]

The presence of quenched disorder is known to force fluctuation-driven first order transitions to become continuous,[23] and this appears to be the case in the thin film sample. While previous studies have found that the crossover from first to second order is complete below ~100 nm in LCMO particles,[12–14] in the present case weak first order characteristics persist in the 33 nm particles. A clearer understanding of the driving force behind the size-induced crossover from first to second order may be necessary before this discrepancy can be explained. In systems displaying a bulk first-order transition, the order parameter may vanish continuously at a free surface leading to divergence of the correlation lengths as in a second order material,[24] and it has been speculated that in nanoparticle systems the first order transition in the core is masked by a second order transition at the disordered surface.[12] Surface-induced pressure on the nanoscale has also been invoked to explain the destabilization of the first order transition,[13] which has an established sensitivity to external and chemical pressure in manganites.[25,26] Alternatively, it was proposed that random local strain fluctuations and bandwidth enhancement act in tandem to change the nature of the transition in manganite nanoparticles.[14] These mechanisms, particularly those based on surface effects, suggest that the critical size for the establishment of the second order transition may be strongly influenced by the details of the sample morphology. Indeed, Tang *et al.* reported the absence of a first order signature in Arrott plot slopes below 160 nm, while Hueso *et al.* observed negative slopes for 95 nm particles. In the present case, the weak first order nature seen in 33 nm particles may be an effect of strong agglomeration, although we note that the breakdown of universal behavior is more sensitive to the presence of a first order contribution than Arrott plots alone.[22]

In summary, the magnetic and magnetocaloric properties of bulk polycrystalline, nanocrystalline, and thin film samples of the CMR manganite $La_{0.7}Ca_{0.3}MnO_3$ were investigated to observe the effects of reduced dimensionality in the system. Broadened transitions along with reduced Curie temperature, magnetic moment, and magnetic entropy change were observed in the nanocrystalline and thin film samples. Interestingly, the properties of the 150 nm film showed greater deviation from the bulk than those of the 33 nm nanoparticles, with properties more closely matched to those of the 15 nm particles. Notably, however, the film exhibited enhanced refrigerant capacity over the polycrystalline and nanocrystalline samples. The first order transition in bulk LCMO is weakened in the 33 nm nanoparticles and converted to second order in the thin film and smallest particle size.

The work at the University of South Florida was supported by DOE BES Physical Behavior of Materials Program through Grant No. DE-FG02-07ER46438. P.L. acknowledges support from the University of South Florida's Presidential Doctoral Fellowship. M.H.P. acknowledges support from the Florida Cluster for Advanced Smart Sensor Technologies (FCASST). H.K., M.O., and A.P. acknowledge support from the Office of Naval Research. S.C.Y. and T.L.P. acknowledge support from the Converging Research Center Program funded by the Ministry of Education, Science and Technology (2012K001431).

[1]O. Gutfleisch, M. A. Willard, E. Bruck, C. H. Chen, S. G. Sankar, and J. P. Liu, Adv. Mater. **23**, 821 (2011).
[2]Y. Tokura, Rep. Prog. Phys. **69**, 797 (2006).
[3]Y. A. Soh, G. Aeppli, N. D. Mathur, and M. G. Blamire, Phys. Rev. B **63**, 020402 (2000).
[4]P. K. Siwach, H. K. Singh, and O. N. Srivastava, J. Phys. Condens. Matter **18**, 9783 (2006).
[5]J. Dvorak, Y. U. Idzerda, S. B. Ogale, S. Shinde, T. Wu, T. Venkatesan, R. Godfrey, and R. Ramesh, J. Appl. Phys. **97**, 10C102 (2005).
[6]M. Egilmez, K. H. Chow, and J. Jung, Appl. Phys. Lett. **92**, 162515 (2008).
[7]M. Ziese, H. C. Semmelhack, K. H. Han, S. P. Sena, and H. J. Blythe, J. Appl. Phys. **91**, 9930 (2002).
[8]A. de Andres, J. Rubio, G. Castro, S. Taboada, J. L. Martinez, and J. M. Colino, Appl. Phys. Lett. **83**, 713 (2003).
[9]D. Kim, B. Revaz, B. L. Zink, F. Hellman, J. J. Rhyne, and J. F. Mitchell, Phys. Rev. Lett. **89**, 227202 (2002).
[10]A. N. Ulyanov, Y. M. Kang, and S. I. Yoo, J. Appl. Phys. **103**, 07B328 (2008).
[11]D. H. Manh, P. T. Phong, T. D. Thanh, D. N. H. Nam, L. V. Hong, and N. X. Phuc, J. Alloys Compd. **509**, 1373 (2011).
[12]L. E. Hueso, P. Sande, D. R. Miguens, J. Rivas, F. Rivadulla, and M. A. Lopez-Quintela, J. Appl. Phys. **91**, 9943 (2002).
[13]W. Tang, W. J. Lu, X. Luo, B. S. Wang, X. B. Zhu, W. H. Song, Z. R. Yang, and Y. P. Sun, J. Magn. Magn. Mater. **322**, 2360 (2010).
[14]T. Sarkar, A. K. Raychaudhuri, A. K. Bera, and S. M. Yusuf, New J. Phys. **12**, 123026 (2010).
[15]P. Dey, T. K. Nath, P. K. Manna, and S. M. Yusuf, J. Appl. Phys. **104**, 103907 (2008).
[16]H. Kim, M. Osofsky, R. C. Y. Auyeung, and A. Pique, Appl. Phys. Lett. **100**, 142403 (2012).
[17]J. Curiale, M. Granada, H. E. Troiani, R. D. Sanchez, A. G. Leyva, P. Levy, and K. Samwer, Appl. Phys. Lett. **95**, 043106 (2009).
[18]N. S. Bingham, M. H. Phan, H. Srikanth, M. A. Torija, and C. Leighton, J. Appl. Phys. **106**, 023909 (2009).
[19]A. M. Pereira, J. C. R. E. Oliveira, J. C. Soares, J. Ventura, J. B. Sousa, and J. P. Araujo, J. Non-Cryst. Solids **354**, 5295 (2008).
[20]X. Moya, L. E. Hueso, F. Maccherozzi, A. I. Tovstolytkin, D. I. Podyalovskii, C. Ducati, L. C. Phillips, M. Ghindini, O. Hovorka, A. Berger, M. E. Vickers, E. Defay, S. S. Dhesi, and N. D. Marthur, Nature Mater. **12**, 52–58 (2012).
[21]C. M. Bonilla, F. Bartolome, L. M. Garcia, M. Parra-Borderias, J. Herrero-Albillos, and V. Franco, J. Appl. Phys. **107**, 09E131 (2010).
[22]C. M. Bonilla, J. Herrero-Albillos, F. Bartolome, L. M. Garcia, M. Parra-Borderias, and V. Franco, Phys. Rev. B **81**, 224424 (2010).
[23]S. Rossler, U. K. Rossler, K. Nenkov, D. Eckert, S. M. Yusuf, K. Dorr, and K. H. Muller, Phys Rev B **70**, 104417 (2004).
[24]L. Turban and F. Igloi, Phys. Rev. B **66**, 014440 (2002).
[25]P. Sarkar, S. Arumugam, P. Mandal, A. Murugeswari, R. Thiyagarajan, S. E. Muthu, D. M. Radheep, C. Ganguli, K. Matsubayshi, and Y. Uwatoko, Phys. Rev. Lett. **103**, 057205 (2009).
[26]M. H. Phan, V. Franco, N. S. Bingham, H. Srikanth, N. H. Hur, and S. C. Yu, J. Alloys Compd. **508**, 238 (2010).